Available online at www.sciencedirect.com
SCIENCE DIRECT®
Journal of Power Sources 133 (2004) 52–58
JOURNAL OF POWER SOURCES
www.elsevier.com/locate/jpowsour

Effect of barium sulfate and strontium sulfate on charging and discharging of the negative electrode in a lead–acid battery

H. Vermesan [a,*], N. Hirai [a], M. Shiota [b], T. Tanaka [a]

[a] *Department of Materials Science and Processing, Graduate School of Engineering, Osaka University, Yamadaoka 2-1, Suita, Osaka 565-0871, Japan*
[b] *Yuasa Corporation, 2-3-21 Kosobe-cho, Takatsuki, Osaka 569-1115, Japan*

Received 7 August 2003; accepted 30 November 2003

Abstract

A fundamental study is undertaken of the mechanism of the formation and dissolution of lead sulfate on the negative electrode in a lead–acid battery. This involves in situ examination of a lead sheet, on which a small amount of $BaSO_4$ or $SrSO_4$ powder is fixed by pressing, in sulfuric acid solution by means of electrochemical atomic force microscopy (EC-AFM) combined with cyclic voltammetry (CV). It is found that both $BaSO_4$ and $SrSO_4$ provide seed crystals for the precipitation of $PbSO_4$. The $PbSO_4$ crystals are formed more rapidly on $SrSO_4$ than on $BaSO_4$ during the oxidation (discharge) process. The dissolution of $PbSO_4$ crystals formed on $SrSO_4$ crystals is very slow during the reduction (charge) process.

Keywords: Barium sulfate; Cyclic voltammetry; Electrochemical atomic force microscopy; Lead–acid battery; Negative electrode; Strontium sulfate

1. Introduction

The effect of inorganic additives in the negative electrode of lead–acid batteries has been reported by several investigators [1–4]. The use of additives in the active material (sponge lead) can increase the performance of the electrode under cycling service. A negative electrode can lose performance due to passivation of the surface (deposition of an impermeable film of lead sulfate on the lead substrate). The negative electrodes in lead–acid batteries must have sufficient porosity to assure a good contact area between lead and electrolyte. In the absence of additives, the porosity rapidly diminishes on cycling. This adverse behavior can be ameliorated through the use of additives.

Strontium sulfate ($SrSO_4$) and barium sulfate ($BaSO_4$) are electrochemically inactive and insoluble in sulfuric acid. Due to these properties, the two compounds remain chemically unchanged in the negative electrode. The sulfates of barium, strontium and lead are similar in crystalline form (isostructural) [5]. By virtue of these qualities, the compounds are considered to act as sites for the precipitation of lead sulfate ($PbSO_4$) during discharge. Although the application of barium is well known and $SrSO_4$ has been shown to be effective [6], there is still considerable uncertainty about the detailed mechanism of the effect of these two inorganic additives.

The aim of this investigation is to observe, in situ, the mechanism of formation and dissolution of $PbSO_4$ crystals on negative electrodes doped with inorganic additives. Previously, the formation of $PbSO_4$ has been studied by means of a scanning electron microscopy (SEM) and other techniques. The use of electrochemical atomic force microscope (EC-AFM) [7–13] allows examination of the intimate phenomena that occur on the surface of lead negative electrodes using $BaSO_4$ or $SrSO_4$ as additives. With this technique, it has become possible to see how the sulfate crystals are formed on the surface, how they grow, and how they appear. This assists greatly the understanding of the complex processes that occur at the electrode|electrolyte interface in a lead–acid battery. The study reported here provides new information on the mechanism of the reactions that take place on the surface of the lead electrode.

2. Experimental

2.1. Equipment

The effects of $BaSO_4$ and $SrSO_4$ on the negative electrode of a lead–acid battery were examined in situ by means of the EC-AFM arrangement shown schematically in Fig. 1.

* Corresponding author. Permanent address: Technical University of Cluj-Napoca, Osaka 565-0871, Japan. Tel.: +81-6-6879-7467; fax: +81-6-6879-7467.
E-mail address: horatiu.vermesan@mat.eng.osaka-u.ac.jp (H. Vermesan).

0378-7753/$ – see front matter © 2004 Elsevier B.V. All rights reserved.
doi:10.1016/j.jpowsour.2003.11.071

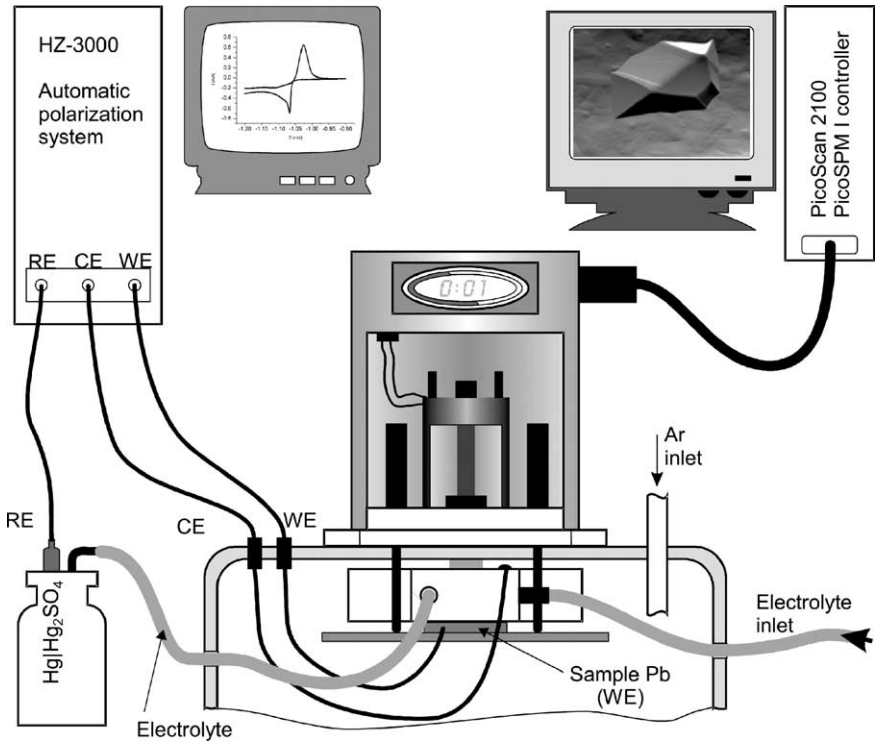

Fig. 1. Schematic representation of experimental equipment.

This is composed of a microscope (PicoSPM) and a controller (PicoScan 2100) made by Molecular Imaging (MI Co.). EC-AFM observations were performed with a commercial Si_3N_4 cantilever that had integral gold-coated tips. Cyclic voltammetry (CV) was performed with an Automatic Polarization System, HZ-3000, made by Hokuto Denko Co. The electrochemical cell, which is shown schematically in Fig. 2, comprised a lead working electrode, a PbO_2 counter electrode, and a $Hg|Hg_2SO_4$, 50 mM H_2SO_4 reference electrode. All potentials are reported with respect to this electrode.

2.2. Preparation of EC-AFM cell

The negative electrode was a pure-lead sheet (99.99%), and the electrolyte was 5 M H_2SO_4. Oxygen dissolved in the electrolyte was removed by bubbling argon gas through the cell for more than 2 h prior to experiment. The lead was

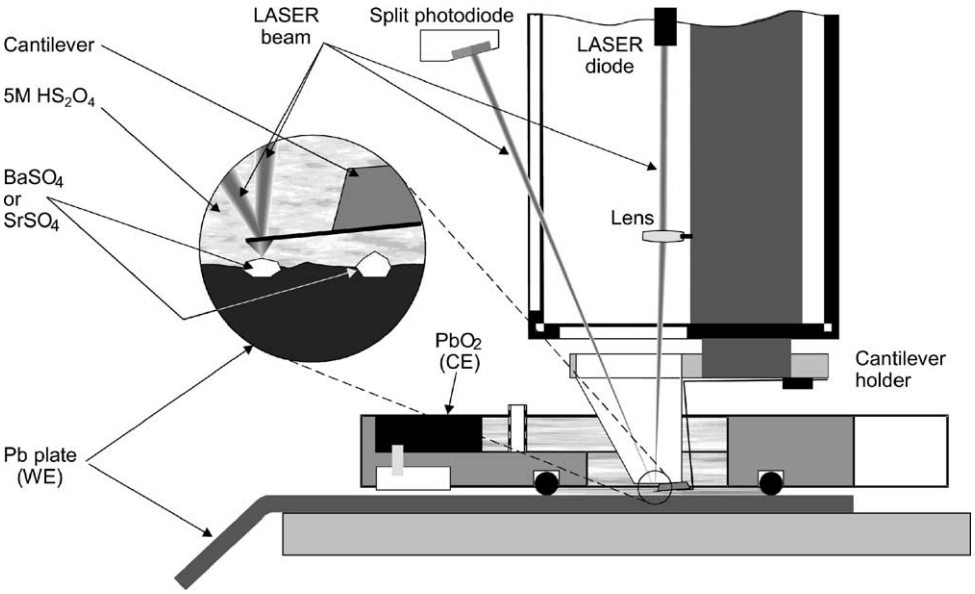

Fig. 2. Electrochemical cell and cantilever set-up.

cleaned with acetic acid to remove the surface layer of lead oxide, and then washed with ethanol. After preparing the surface of the electrode, a small amount of $BaSO_4$ or $SrSO_4$ powder was pressed on the surface. For EC-AFM observations, three types of samples were prepared, namely: (i) without any additives (lead plates); (ii) with $BaSO_4$ powder; (iii) with $SrSO_4$ powder. The electrode was placed in the test cell and had an exposed area of about 1.25 cm^2. In order to reduce any oxides on the lead surface, a negative potential was applied in two steps: −1400 mV for 10 min followed by −1200 mV for 10 min, as shown in Fig. 3.

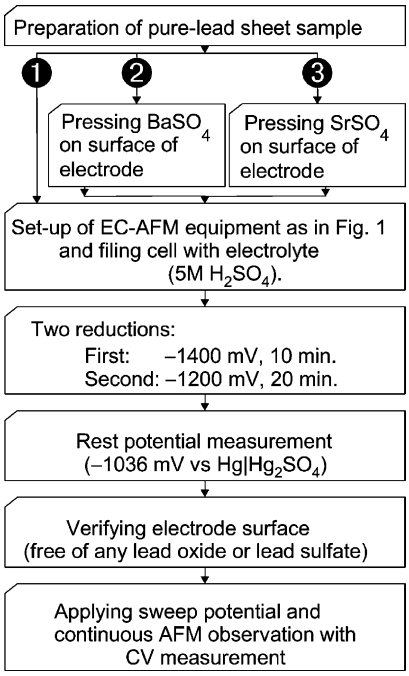

Fig. 3. Step-by-step operations for AFM observations with CV measurements.

3. Results and discussions

Image analysis was performed with The Scanning Probe Image Processor (SPIP™) which contains many generic analytical and visualization tools for correcting and analyzing data from atomic force microscopy.

3.1. Effect of $BaSO_4$

The stages (potential–time) where AFM images were taken are shown on the current–time plots in Fig. 4. The

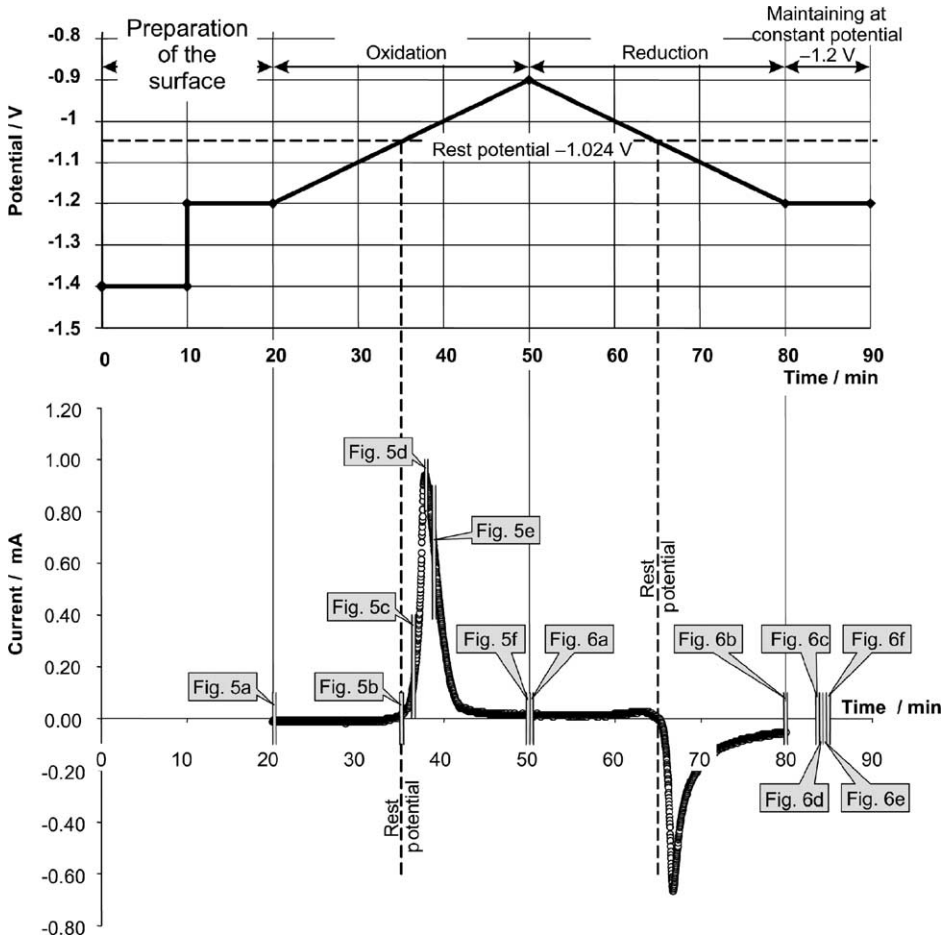

Fig. 4. Conditions (potential-time) and stages on the time–current plot where AFM images for Figs. 5 and 6 were taken.

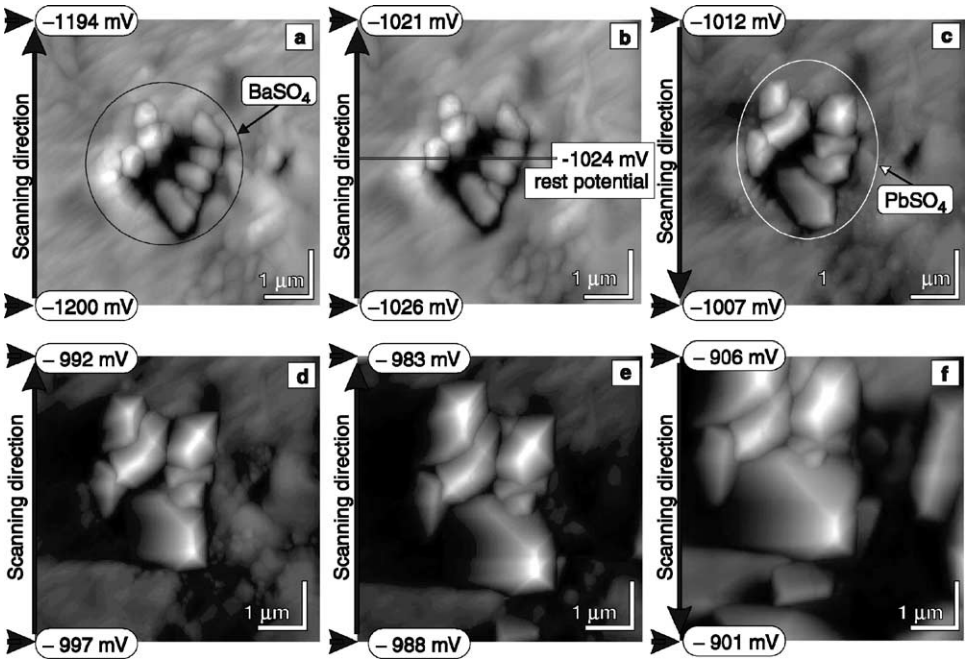

Fig. 5. Oxidation of negative electrode with $BaSO_4$ as additive: (a) image of initial $BaSO_4$ crystals on lead surface at beginning of oxidation (discharge); (b) point where potential reaches rest potential; (c)–(e) formation and growth of $PbSO_4$ on $BaSO_4$ crystals; (f) end of oxidation.

AFM images obtained during oxidation (discharge) of the negative electrode are given in Fig. 5. The experiments confirm that $PbSO_4$ starts to crystallize preferentially on the $BaSO_4$ seed crystals due the close similarity in the structures of the two compounds (Table 1). The crystallization of $PbSO_4$ becomes very fast at potentials less negative than the rest potential (−1024 mV). The initial growth rate is low, but increases as the potential sweep proceeds in a positive-going direction. AFM images obtained during reduction (charge) of the negative electrode are presented in Fig. 6. The experiments demonstrate that only a small amount of $PbSO_4$ is dissolved after the potential reaches −1024 mV (rest potential). Crystals of $PbSO_4$ are still present when the potential reaches −1200 mV (Fig. 6(b)). After about 3 min at this po-

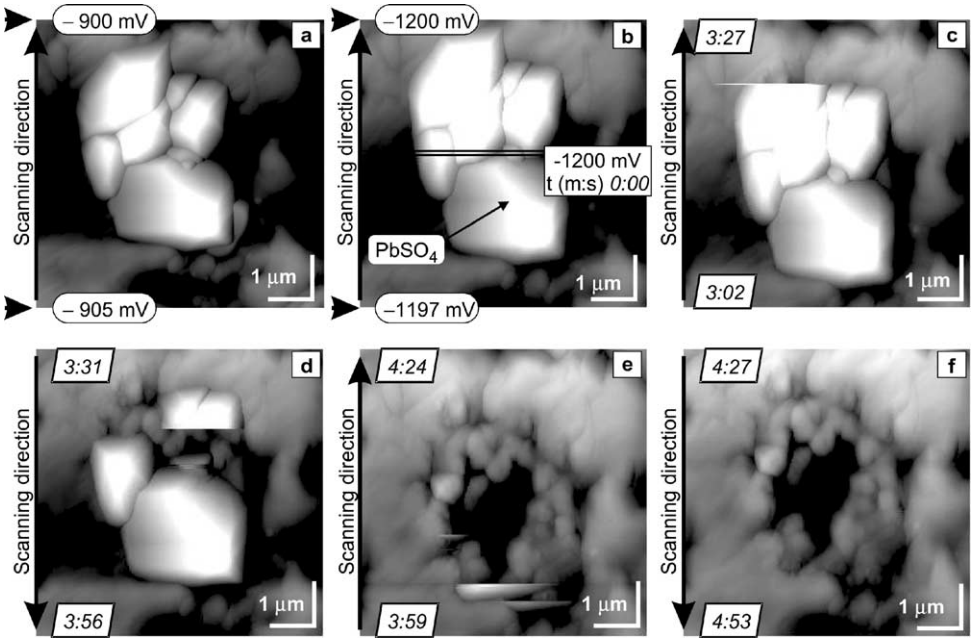

Fig. 6. Reduction of negative electrode with $BaSO_4$ as additive: (a) image of $PbSO_4$ crystals at beginning of reduction phase; (b) image of crystal immediately after potential reaches −1200 mV; (c) beginning of dissolution of $PbSO_4$ crystals about 3 min after potential reaches −1200 mV; (d) process of dissolution of lead sulfate; (e) end of dissolution of lead sulfate, after less than 1 min from beginning of dissolution; (f) image of surface after reduction. Seed crystals of $BaSO_4$ are dragged with $PbSO_4$ into H_2SO_4 solution.

Table 1
Cell dimensions and axial ratios (a:b:c) for $BaSO_4$, $SrSO_4$ and $PbSO_4$

Cell dimensions	$BaSO_4$ (barite)	$SrSO_4$ (celestine)	$PbSO_4$ (anglesite)
a	8.878	8.359	8.48
b	5.45	5.352	5.398
c	7.152	6.866	6.958
a:*b*:*c*	1.6289:1:1.3122	1.5618:1:1.2828	1.5709:1:1.2889

Source: Mineralogy Database http://webmineral.com/data/.

tential, the dissolution of $PbSO_4$ commences and the reaction is very fast (Fig. 6(c)), and after about 4 min the crystals are removed (reduced) from the lead surface (Fig. 6(e)). The location of the initial crystals of $BaSO_4$ is shown in Fig. 6(f). It can be seen that the $BaSO_4$ is removed from the surface together with the $PbSO_4$ during the reduction phase.

3.2. Effect of $SrSO_4$

The experimental conditions were the same as those for the $BaSO_4$ study. The stages where AFM images were taken on the time–current plot during oxidation and reduction of the negative electrode are indicated in Fig. 7. Those for oxidation (discharge) of the negative electrode are given in Fig. 8. It is confirmed that the lead sulfate starts to grow on the $SrSO_4$ crystals. The initial crystallization of $SrSO_4$ is very fast, before reaching the rest potential. The lattice parameters of $SrSO_4$ are almost similar to those of $PbSO_4$, as shown in Table 1. This close similarity offers crystallization seeds for $PbSO_4$ and the experiments indicate that $PbSO_4$ will form more rapidly on $SrSO_4$ than on $BaSO_4$. Evolution of $PbSO_4$ crystals during reduction (charge) is shown in Fig. 9. In this case, after the potential reaches −1200 mV, the $PbSO_4$ is not completely reduced from the surface. As in the previous experiments, a constant potential (−1200 mV) was maintained in order to determined the time that it takes for $PbSO_4$ to be dissolved. It is found that after almost 1 h, the $PbSO_4$ crystals are not dissolved from the surface (Fig. 9(f)). It is concluded that, in the presence of $SrSO_4$, formation of the $PbSO_4$ during discharge is faster, but dissolution during charge is slower. Thus, the $PbSO_4$ crystals formed on $SrSO_4$ are very stable and difficult to dissolve in the electrolyte.

In the both cases, the formation and growth of the $PbSO_4$ crystals is not uniform on the surface. The $PbSO_4$ starts

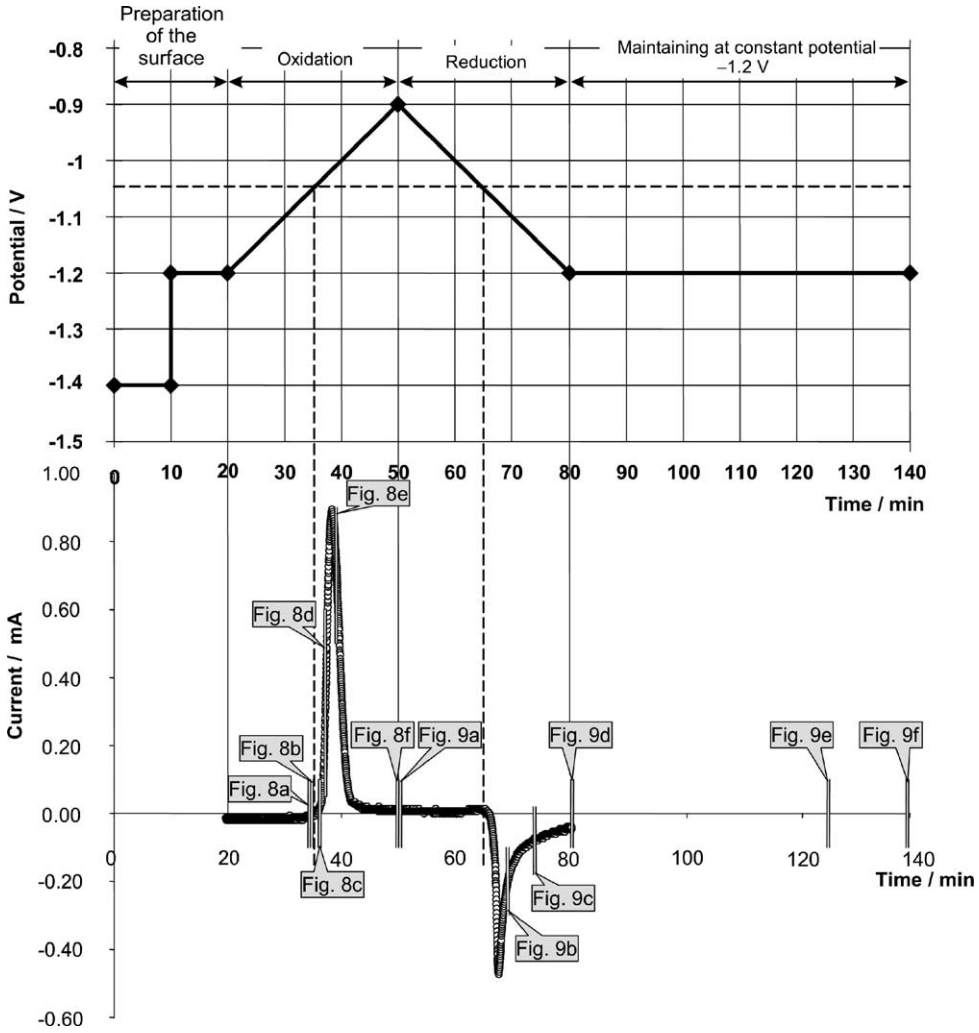

Fig. 7. Conditions (potential–time) and stages on time–current plot where AGM images were taken during oxidation and reduction of negative electrode.

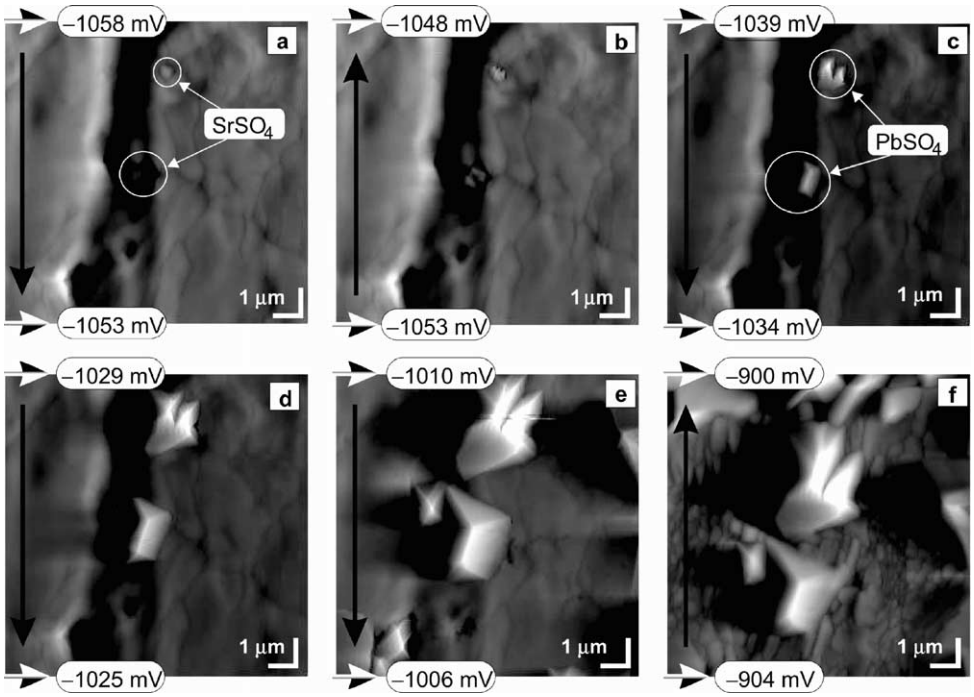

Fig. 8. Oxidation of negative electrode with $SrSO_4$ as additive; (a) image of two small $SrSO_4$ crystals on surface of lead electrode before current becomes positive; (b) beginning of crystallization of $PbSO_4$ crystals, the potential is still under the rest potential, but the current is positive; (c)–(e) evolution of lead sulfate on surface of electrode; (f) end of oxidation.

to crystallize on $BaSO_4$ or $SrSO_4$ but the area around the $BaSO_4$, or $SrSO_4$ crystals remains free of any $PbSO_4$ crystals. Therefore, additives like $BaSO_4$ or $SrSO_4$ eliminate (or suppress) 'coating' of the lead active mass.

4. Conclusions

This study has given rise to the following observations.

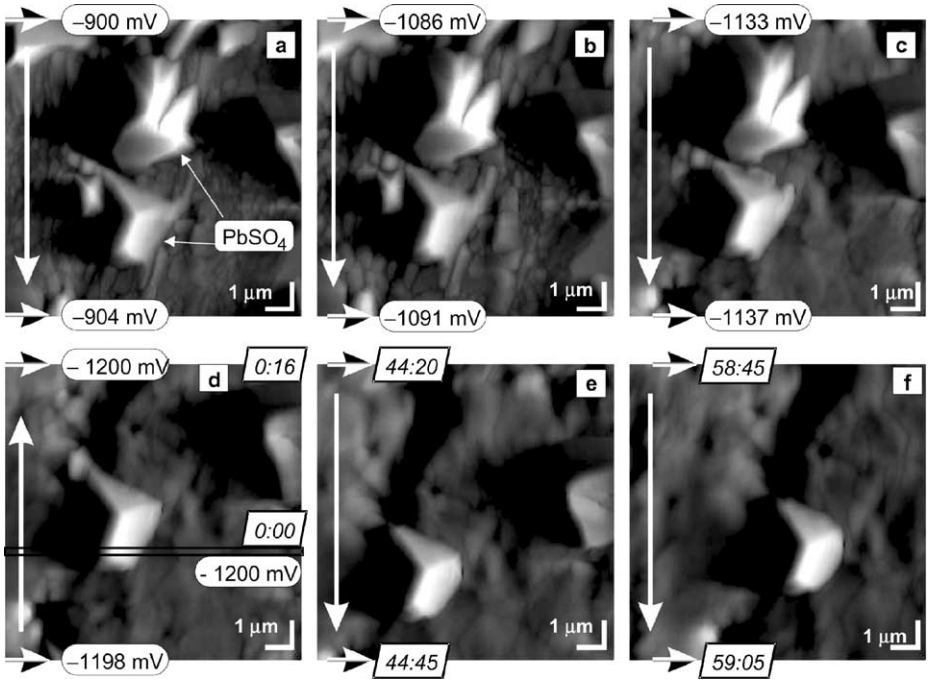

Fig. 9. Reduction of negative electrode with $SrSO_4$ as additive: (a) beginning of reduction (charging) phase, potential goes to negative values; (b)–(c) process of dissolution of $PbSO_4$ crystals; (d) point where potential reaches −1200 mV, end of reduction period; (e) AFM image of $PbSO_4$ after about 44 min after potential reaches −1200 mV; (f) image of lead surface with $PbSO_4$ crystals after almost 1 h at −1200 mV.

(i) Inorganic additives such as $BaSO_4$ or $SrSO_4$ promote the precipitation of $PbSO_4$ on lead electrodes.
(ii) During discharge, $PbSO_4$ is formed very rapidly on $SrSO_4$ crystals (before reaching the rest potential) and is very difficult to dissolve during the charge process.
(iii) $PbSO_4$ crystallizes on $BaSO_4$ or $SrSO_4$ seeds and the surrounding regions remain free of $PbSO_4$ crystals. This will prevent 'coating' or passivation of the active mass.

The study has demonstrated that EC-AFM is a powerful tool for observing and studying the intimate processes that occur at the surface of the negative electrode in a lead–acid battery during the charge and the discharge processes.

Acknowledgements

The authors are grateful to Prof. Hara of Osaka University for his support and useful discussion of this work. The study was partly supported by the Industrial Technology Research Grant Program (ID number: 01B60015C) in 2001–2003 from the New Energy and Industrial Technology Development Organization (NEDO) of Japan.

References

[1] D.P. Boden, J. Power Sources 73 (1998) 89–92.
[2] G.W. Vinal, Storage Batteries, Wiley, New York, USA 1947.
[3] G. Sterr, Electrochim. Acta 15 (1970) 1221.
[4] B.N. Kabanov, in: Proceedings of the 3rd Conference on Electrochemistry, Moscow, Russia, 1953, p. 138.
[5] M. Miyake, H. Morikawa, I. Minato, S.-I. Iwai, Am. Mineralogist 63 (1978) 506–510.
[6] A.K. Lorenz, Dissertation, Leningrad, Russia, 1953.
[7] Y. Yamaguchi, M. Shiota, Y. Nakayama, N. Hirai, S. Hara, J. Power Sources 85 (2000) 22–28.
[8] Y. Yamaguchi, M. Shiota, Y. Nakayama, N. Hirai, S. Hara, J. Power Sources 93 (2001) 104–112.
[9] M. Shiota, Y. Yamaguchi, Y. Nakayama, K. Adachi, S. Taniguchi, N. Hirai, S. Hara, J. Power Sources 95 (2001) 203–208.
[10] Y. Yamaguchi, M. Shiota, Y. Nakayama, M. Hosokawa, N. Hirai, S. Hara, J. Power Sources 102 (2001) 156–162.
[11] I. Ban, Y. Yamaguchi, Y. Nakayama, N. Hirai, S. Hara, J. Power Sources 107 (2002) 167–172.
[12] M. Shiota, Y. Yamaguchi, Y. Nakayama, N. Hirai, S. Hara, J. Power Sources 113 (2003) 277–280.
[13] N. Hirai, K. Takeda, S. Hara, M. Shiota, Y. Yamaguchi, Y. Nakayama, J. Power Sources 113 (2003) 329–334.